

## NUMERICAL ESTIMATION OF FUEL LOSS CAUSED BY SELF-IGNITION AND APPLICATION TO COAL FIRE PROPAGATION IN INCLINED SEAM

**Yanming Wang**

School of Safety Engineering,  
China University of Mining and  
Technology  
Xuzhou, Jiangsu, China

**Wujun Song**

School of Safety Engineering,  
China University of Mining and  
Technology  
Xuzhou, Jiangsu, China

**Zhixiong Guo**

Department of Mechanical and  
Aerospace Engineering,  
Rutgers, The State University of  
New Jersey  
Piscataway, NJ, USA

### ABSTRACT

All the headings should be uppercase, bold Arial size 10 font. In order to comprehensively understand the serious disaster of underground mineral self-ignition and source loss in practice, dynamical and thermo-chemical phenomena of coal spontaneous combustion were investigated. A coupled conductive, convective and radiative heat transfer model for inclined outcrop seam in porous coal-bearing stratum with transient exothermic source term was established. Combined with models of coal oxidation, oxygen supplement and fuel consumption, the large-scale and long-term history of coal fire was simulated. Recorded data indicate that spontaneous combustion firstly occurs under lean oxygen condition and fire development is mainly controlled by reaction heat release during early oxidation process but by oxygen restriction after coal self-ignition. Considering the variation of influence factors, comparative analyses illustrate that the propagation rate and fuel loss, that reduce when the stratum porosity decreases, are significantly and positively related to the leakage intensity. The presented method and results could provide a useful reference to loss estimation and efficient treatment of nature hazardous.

### NOMENCLATURE

$A$	Frequency factor, Hz
$C_o$	Local oxygen concentration, kg/m <sup>3</sup>
$C_p$	Specific heat, kJ/(kg·K)
$E_a$	Activation energy, kJ/mol
$\vec{g}$	Gravitational vector, m/s <sup>2</sup>
$k$	Permeability, m <sup>2</sup>
$O_r$	Theoretical oxygen requirement for combustion, kg/kg coal
$p$	Hydrostatic pressure, Pa
$S$	Compressibility, 1/Pa
$q$	Heat release rate, W/g
$q_r$	Heat flux of radiation, W/m <sup>2</sup>
$Q$	Reaction heat, J/g

$Q_{net}$	Net calorific value of coal, MJ/kg
$R$	Gas constant
$t$	Time, s
$T$	Absolute temperature, K
$v$	Seepage velocity, m/s
$w$	Quantity of local oxygen consumption. Kg/(m <sup>3</sup> ·s <sup>1</sup> )
<i>Greek symbols</i>	
$\beta$	Attenuation coefficient, m <sup>-1</sup>
$\sigma$	Stephan-Boltzmann constant
$\lambda$	Thermal conductivity, W/(m·K)
$\mu$	Air dynamic viscosity, Pa·s
$\rho$	Density, kg/m <sup>3</sup>
$\varphi$	Porosity
<i>Subscripts</i>	
$s$	Solid material
$f$	Leakage air

### INTRODUCTION

Coal fire, referring to large-area spontaneous combustion of underground coal oxidation caused by natural condition or human activities, is a serious disaster associated with coal mining in a long history. Uncontrolled coal fires are widespread in China [1], India [2], Indonesia [3], the United States [4,5], South Africa [6] and distribute throughout the world.

Because of special geographical location, climate condition and artificial factor, some worst disasters of coal fire occur in China with an annual coal loss of 13.6 million tons [7]. Among all the fire areas, Xinjiang region where has the most abundant coal in China suffers the most severe coal fires. According to the latest report issued by Xinjiang Coal Fire Fighting Bureau [8], by the end of 2010, there were 49 coal fire areas in Xinjiang region. About 8,126 kilotons of coal were burned out each year with a burning area of  $9.06 \times 10^6$  m<sup>2</sup> and the direct economic loss was nearly one billion yuan every year.

Coal fire not only consumes the coal resource for nothing, but also brings serious problems to local environment and ecology, such as atmosphere pollution, damage to soils, contamination to underground water and consequently the health problems to human beings [9]. A typical example reported by Xinjiang Coal Fire Fighting Bureau is the Heshituoluogai coal fire [10] that is currently one of the last three State Key Coal fires in Xinjiang province. There are 12 sub-fire areas, distributed in a range of 57 km<sup>2</sup>, and the total area of the fire is approximately 1,443,221 m<sup>2</sup>. Every year, roughly estimated coal loss by self-combustion achieves 1.5 million tons and other more than ten times of fuel sources could not be exploited due to the threat of the nearby underground fires. Besides, more than 2 million tons of greenhouse and toxic gases release from the mining areas every year and greatly deteriorate the air quality of local residence district. Although many efforts to extinguish fires such as water injection and surface covering had been taken place, the coal fires in this region still spread rapidly since it is hard to indicate the movement rate of coal fire or position of combustion core accurately.

Generally speaking, coal fire research mainly involves two aspects: one is the mechanisms of fire ignition, development and propagation, focusing on the causes of coal fire and combustion evolution; the other is controlling technologies mainly including fire areas detection, monitoring and extinguishing methods and materials. The thermodynamic characteristic of self-combustion system is a key in the research of coal fire because of its roles in revealing the mechanism of fire propagation and fuel consumption as well as scientifically evaluating the environmental impacts. Previous reports [11, 12] pointed out that underground coal fire is a multidisciplinary physical and chemical process cross the complicated coal-oxygen reactions, seepage flow and gas dispersion, and coupled heat and mass transfer.

For coal fire prevention and control, studies [13, 14] have been carried out on thermal efficiency enhancement, pollution control of coal burning, coal oxidation and combustion properties by low-temperature oxidation experimental systems, including physical and chemical adsorption mechanism, equations of coal and oxygen reactions and kinetic parameters (thermal conductivity, reaction heat, activation energy and former factor, etc.) under natural heating conditions. These micro-level results could help the analyses of coal combustion characteristics. However, it is hard to describe the real state of underground coal combustion in large scale by using the theory of coal oxidation directly, because laboratory-scale results of kinetic properties could not be transferred to simulating model of spontaneous combustion process uncritically. In fact, field coal combustion or heat release is not only determined by reaction rate but also limited by local oxygen supplement and transport [15]. That means the quantitative correlation between oxygen requirements and fuel consumption needs to be concerned in estimating the real coal combustions process under these aforementioned conditions.

In order to understand the thermodynamic characteristics of fire propagation and reserves loss, a numerical study is carried

out in this paper. The dependence of heat release rate from coal oxidation on oxygen supply is investigated at first, and then the coal and oxygen consumption model is established with the quantitative correlation between theoretical oxygen requirements and coal elements. Based on the principles of heat and mass transfer in porous medium, the coupled heat transfer model for underground combustion system of coal fire development is presented with proper boundary and initial conditions as well as thermo-chemical and physical parameters. The profiles of fire history are traced and the consumptions of coal reserves and oxygen are discussed at different stages in the fire development. Analysis of influencing factors including inclined angle, leakage intensity and porosity is implemented. Finally, a typical coal fire in Heshituoluogai fire areas is taken into account in the simulation, and the coal loss and fire advancing rate are predicted and compared with results from other indirect methods.

## THEORY AND SIMULATION MODEL

### Fuel consumption and reaction heat

Fuel consumption rate and heat release intensity of coal combustion have crucial influences on continuous burning in coal fire development. Both factors are regarded as inner motive power for combustion front propagation and key parameters of thermodynamic characteristics.

As so far, the exothermic reaction of fossil fuel and its kinetic parameters have been widely identified in energy chemical industry. For coal oxidation, according to the kinetics theory of coal-oxygen reaction [16], the exothermal capacity of coal related to the reaction rate at different temperatures can be written as:

$$q(T) = QAe^{-E_a/RT} \quad (1)$$

where  $q(T)$  is the heat release rate per unit mass at absolute temperature  $T$ ,  $R$  is the universal gas constant,  $E_a$ ,  $A$  and  $Q$  are the activation energy, the frequency factor and reaction heat, respectively. These kinetic parameters could be obtained by thermo gravimetric (TG) and differential scanning calorimetry (DSC) measurements [17] in laboratory. Integrating the exothermal capacity through the whole reaction process from ambient temperature to burnout, the total heat release or net calorific value of coal  $Q_{net}(= \int q(T)dt)$  could be estimated. Between the interval time  $t$  to  $t+\Delta t$  with varying temperature, the amount of coal consumption reads

$$\Delta\rho_t = \rho_s \int_t^{t+\Delta t} q(T)dt/Q_{net} \quad (2)$$

where  $\rho_s$  represents the true related density of local solid fuel.

It should be pointed out that this value represents the theoretical fuel consumption with enough oxygen in the reaction. Unlike laboratory conditions with stable and continuous oxygen supplements, however, the real situation of underground coal combustion is that oxygen supply vis-à-vis rich occurrences of

fuel in the coal seam usually do not guarantee completely burning in fire zone with high temperature. That means oxygen supply or transport is certainly a limiting process of coal oxidation regime and the results of measurements could not be uncritically transferred to developed model simulating spontaneous combustion process of coal underground.

For this aspect, theoretical oxygen requirement  $O_r$  for complete combustion as kg/kg coal is involved in the simulation that can be readily obtained in one step following the overall combustion equation as follows [18]:

$$O_r = 0.08(C/3 + H) + 0.01(S - O) \quad (3)$$

where, C, H, S and O denote the usual notations for carbon, hydrogen, sulphur and oxygen weight percentages (wt%) in a coal on the dry mineral matter free basis, respectively. Thus, the critical fuel consumption related to the theoretical oxygen requirement can be regarded as  $C_o/O_r$ , where  $C_o$  in  $\text{kgm}^{-3}$  is the local oxygen concentration determined by gas diffusion and component producing or consuming rate [19]. Considering these two conditions mentioned above, local coal consumption in field circumstance is given as

$$\Delta\rho_l = \text{Max}(\Delta\rho_t, \frac{C_o}{O_r}) \quad (4)$$

Then, the total consumption or local fuel loss in the coal seam could be obtained by accumulating the local coal consumptions as  $\rho_l = \sum_0^t \Delta\rho_l$ . Meanwhile, along with the fuel consumption, the density of the remaining or residual coal left in the seam which decreases gradually till the coal burns out is easily presented as  $\rho_r = \rho_s - \rho_l$ .

### Coupled heat transfer model

The coupled heat transfer model of underground coal fire is referred to the theory of transport phenomena in porous medium [20]. For the mixed medium consisted of gas and solid material, the two-phase heat transfer equations should be established respectively.

Define the porosity  $\varphi$  as the ratio of fluid volume in total volume. For the leakage air flowing through the pore structure, ignoring the heat source term and expansion work of air, the transient heat transfer equation of gas phase could be written as below.

$$\varphi\rho_f C_{Pf} \frac{\partial T_f}{\partial t} + \rho_f C_{Pf} \vec{v} \cdot \nabla T_f + \varphi \nabla \cdot (q_f) = 0 \quad (5)$$

where  $\rho_f$ ,  $C_{Pf}$  and  $\vec{v}$  are the density, specific heat and seepage velocity of fluid, respectively.  $q_f (= -\lambda_f \nabla T_f - h(T_f - T_s) + \overline{q_{rf}})$  represents the total heat flux in fluid including thermal conduction, convection and radiation.

In the same way, the equation of solid phase could be described as follow:

$$(1 - \varphi)\rho_s C_{Ps} \frac{\partial T_s}{\partial t} + (1 - \varphi)\nabla \cdot (q_s) = (1 - \varphi)\rho_r q(T_s) \quad (6)$$

where  $\rho_s$  and  $C_{Ps}$  are the density and specific heat of coal or rock, respectively.  $q_s (= -\lambda_s \nabla T_s - h(T_s - T_f) + \overline{q_{rs}})$  represents the total heat flux in solid and  $\rho_r q(T_s)$  is reaction heat source which have been described above.

It assumes thermal equilibrium between the solid matrix and gas; and thus, the temperatures of gas and solid materials are regarded as the same. Therefore, combining these two equations, the two-phase energy conservation equation is formulated as:

$$\begin{aligned} & [(1 - \varphi)\rho_s C_{Ps} + \varphi\rho_f C_{Pf}] \frac{\partial T}{\partial t} + \rho_f C_{Pf} \vec{v} \cdot \nabla T = \\ & \nabla \cdot (\lambda_e \nabla T - \overline{q_{re}}) + (1 - \varphi)\rho_r q(T) \end{aligned} \quad (7)$$

where  $\lambda_e (= [(1 - \varphi)\lambda_s + \varphi\lambda_f])$  and  $\overline{q_{re}} (= (1 - \varphi)\overline{q_{rs}} + \varphi\overline{q_{rf}})$  are defined as the effective conductive coefficient and radiation heat flux, respectively. In addition, the radiation heat flux is proportional to  $T^4$  and the temperatures of two phase are regarded as the same, so the radiation heat flux of gas is assumed equal as the solid that  $\overline{q_{re}} = \overline{q_{rs}}$ .

Furthermore, the seepage flow through the coal and rock strata is assumed to behave as Darcy laminar flow in porous medium [21], in which the velocity can be expressed as

$$\vec{v} = \frac{k}{\mu} (\nabla p - \rho_f \vec{g}) \quad (8)$$

where  $k$  in  $\text{m}^2$  is permeability in porous coal or rock,  $\mu$  is air dynamic viscosity and set to be  $1.8 \times 10^{-5} \text{ Pa}\cdot\text{s}$ ,  $p$  is hydrostatic pressure in Pa, and  $\vec{g}$  in  $\text{m}\cdot\text{s}^{-2}$  represents the gravitational vector. Here, the local permeability in the collapsed zone is directly determined by relevant porosity  $\varphi$  varying from 0.1 to 0.4 [22] as follows:

$$k = \frac{k_0}{0.241} \left[ \frac{\varphi^3}{(1 - \varphi)^2} \right] \quad (9)$$

where the initial permeability,  $k_0$ , is given a value of  $10^{-10} \text{ m}^2$ .

### Simulation setup

In this study, a combustion system in inclined outcrop seam of Heshituoluogai coal fires in Xinjiang Regine, China [23] is taken into consideration. As shown in Fig. 1, after original mining in the dip direction at a lower level in the seam, an open and long-strip type goaf along the strike direction is left when coalmine shutdown and then the upper seam is exposed to the leakage air. When the coal temperature rose caused by oxidation, self-ignition would occur almost at the same time through the whole seam in the strike direction and then fire advanced towards the outcrop gradually. Since the fire propagation or movement rate in the strike direction is much greater than that in the dip direction and it can be regarded as infinite, the physical model of underground combustion system is simplified as a two-dimensional section perpendicular to the seam strike including subsidence roof, inclined seam, opened area of goaf and original rock floor.

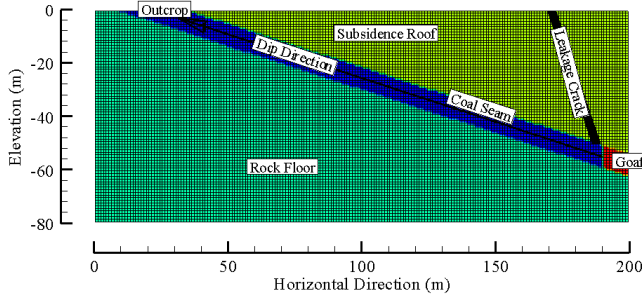


FIG. 1. Physical model of coal-bearing stratum with inclined seam and mesh map.

Based on the geological and uncovering conditions in the coal field, the horizontal scale of simulating strata is set to be 200 m and the whole height from surface to bottom is assumed as 80 m. The thickness of occurrence inclined seam is 8 m and the averaged angle between the dip and horizontal direction approximates  $18^\circ$ . The bottom corner of coal seam is set at 190 m in horizontal direction and 60 m in buried depth. In addition, for inclined mining seam, goaf roof bends and subsides under self and overburden gravity resulting in caving zone occurs. When the tensile stress in rock exceeds the ultimate strength, capping stratum will move down and there exists a vertical fracture belt providing an air-leaking channel in the subsidence roof.

Initial and boundary conditions need to be defined for the temperature, pressure, and gas components. For the temperature, Dirichlet condition is applied for the bottom boundary in which the temperature is assumed 300 K invariably, and Neumann conditions are considered on both sides of the simulation domain and the diffusive flux of thermal energy is assumed zero. Robin boundary condition is applied for the top considering convective heat transfer between rock and the ambient. The ambient temperature and convective heat transfer coefficient are assumed 295 K and  $10 \text{ Wm}^{-2}\text{K}^{-1}$ . For the fluid pressure, it is assumed to be a reference value for all the boundaries under Dirichlet condition. For leakage air, the no-slip conditions are applied on the bottom and both side boundaries. At the surface, there exist a fracture belt in the overlying rock where the air seeps into the seam through the leakage channel and the other part of surface is regarded as seepage exit through the overlying rock and soils. A dominated parameter of fracture width or thickness is considered for the air entrance vent at surface that represents the flow rate. Moreover, an initial temperature at 300 K and hydrostatic pressure distribution are assumed for all the zones in the strata. The relevant pressure referred to standard barometric pressure of 101,325 Pa is directly determined by local geopotential energy at a certain depth. In addition, initial air density of  $1.18 \text{ kgm}^{-3}$  at 300 K with oxygen content of 21 vol% is set in the goaf as well as in the fracture channel.

Furthermore, coal fire is dominated by the physical and mechanical properties (such as density, porosity, permeability rate, compressive strength, etc.) and thermochemical parameters (such as thermal conductivity, heat capacity, reaction rate, heat release, etc.) of coal seam and surrounding rock. These

properties influence the combustion state and propagation of coal fire. In the present case study, according to the field conditions in Heshituoluogai fire areas, the main parameters employed in the simulation are presented as followings. For the chemical properties of coal sample from the fire region, the values of kinetic parameters  $QA$  and  $E_a$  in Eq. (1) could be derived by TG-DSC test [24] so that the heat release can be determined. Here, a two-stage model is involved in the heat source model. For the local coal, the parameters  $QA$  and  $E_a$  below and above the critical temperature  $T_s$  at 598 K are  $3.4 \times 10^5$  and  $1.21 \times 10^6 \text{ W/g}$ , 57.3 and 66.1 kJ/mol, respectively, while the measured ignition temperature reads 725 K. Then, the averaged contents of C, H, O and S elements in the coal sample are obtained as 70.39, 4.39, 23.78 and 0.3 wt% by elemental analysis, respectively, so that the theoretical oxygen requirement for coal combustion is recorded as 1.993 kg/kg coal by using Eq. (3) with net calorific value of  $25.16 \text{ MJkg}^{-1}$ . For the geological parameters, the averaged true relative density of local coal is  $1340 \text{ kgm}^{-3}$  and the surrounding rock density in roof or floor stratum mainly consisted with sandstone is set to be  $2300 \text{ kgm}^{-3}$ . In the simulation, the porosity in the inclined coal seam, subsidence roof and rock floor is set to be 0.2, 0.1 and 0.02, respectively. Especially, the local porosity in the seam is dynamically corrected as the solid density reduces. At surface, the observed width of fractures usually ranges from 1 cm to 20 cm and an averaged value of 10 cm is employed in the simulation. For the thermo-physical parameters, the specific heat capacity of rocks and air is assumed as 2.0 and  $1.0 \text{ kJkg}^{-1}\text{K}^{-1}$ , respectively; the thermal conductivity of coal, rock and air is set to be 0.2, 2.0 and  $0.023 \text{ Wm}^{-1}\text{K}^{-1}$ , respectively. In addition, the diffusion approximation is applied to the radiative heat flux that it can be written as  $\bar{q}_r = -(16\sigma T^3/3\beta)\nabla T$ , in which  $\sigma (= 5.67 \times 10^{-8} \text{ Wm}^{-2}\text{K}^{-4})$  represents the Stephan-Boltzmann constant, and  $\beta$  is the attenuation coefficient of coal and rocks and assumed as  $100 \text{ m}^{-1}$  in the presented simulation.

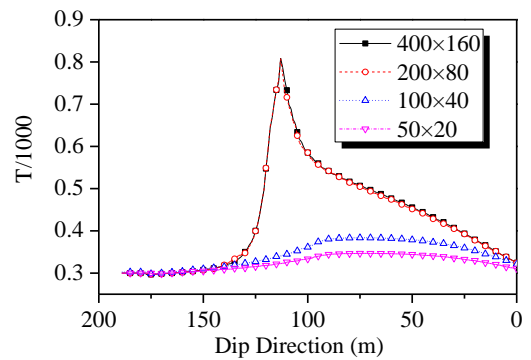


FIG. 2. Simulated temperature distributions along the dip direction with different grid refinement levels.

The finite difference method with the implicit scheme is applied to solve the set of differential equations and the additional source term method is utilized to discrete boundary conditions. A rectangular gridding is carried on the simulation domain, and a series of grid independence study has been implemented to find out optimum grid points in both directions.

The following grid systems are considered 50×20, 100×40, 200×80, 400×160. It has been found that the simulated temperature distribution after 30<sup>th</sup> year at 200×80 grid is extremely close to these results at 400×160 grid as shown in Fig. 2. When more coarse mesh such as 50×20 or 100×40 is carried out, significantly lower temperature is obtained probably due to the omission of original ignition in the seam with large interval. It is concluded that the grid refinement level of 200×80 will be sufficient for the entire calculations, i.e. the grid interval in both directions is set to be 1 m.

## RESULTS AND DISCUSSION

Based on the numerical method and physical model established in the previous work, coupled heat transfer phenomena of coal fire development under spontaneous combustion condition are simulated. The long-term history of coal fire as well as surface heat anomalies are firstly evaluated in the large-scale stratum with inclined coal seam. Then, detailed analyses for the interactions between coal oxidation and ignition, oxygen or fuel consumption and fire propagation are implemented during different periods in the fire development. Moreover, considering the main influent factors such as dip angle of outcrop seam, stratum porosity and seepage velocity, comparative studies on the varying laws of fire propagation are presented in this section.

### Coal fire development

By using the simulation model, the profiles of thermodynamic process of the subsurface coal fire development are recorded as shown in Fig. 3. It draws the time-depended slices of simulated temperature distributions in the two-dimensional strata with outcrop coal seam due to coal fire propagation. The results show that the original temperatures in the coal and surrounding rock stay at a low level for an extremely long time after the seam uncovering due to the tiny heat release from oxidation reaction or chemisorption at low temperature. In this period, with oxygen seeping into the coal gradually in the dip direction, the oxidations perform through the whole seam before the 12<sup>th</sup> year. Then, the accumulated heat at the seam bottom achieves the ignition temperature and naked flame occurs near there. From ignition beginning, the heat flux diffuses from the seam into the upper rock rapidly and the combustion or high temperature zone expand sharply but the temperature of the rest seam near outcrop drops to the ambient value without oxygen supply. During the period from 12<sup>th</sup> to 15<sup>th</sup> year, the range of hotspots enlarges but the movement of combustion center is not apparent yet. After that time, the fire starts to advance towards the seam outcrop. The propagation rate of fire front reads about 40 m for every five years or 8-10 m per year.

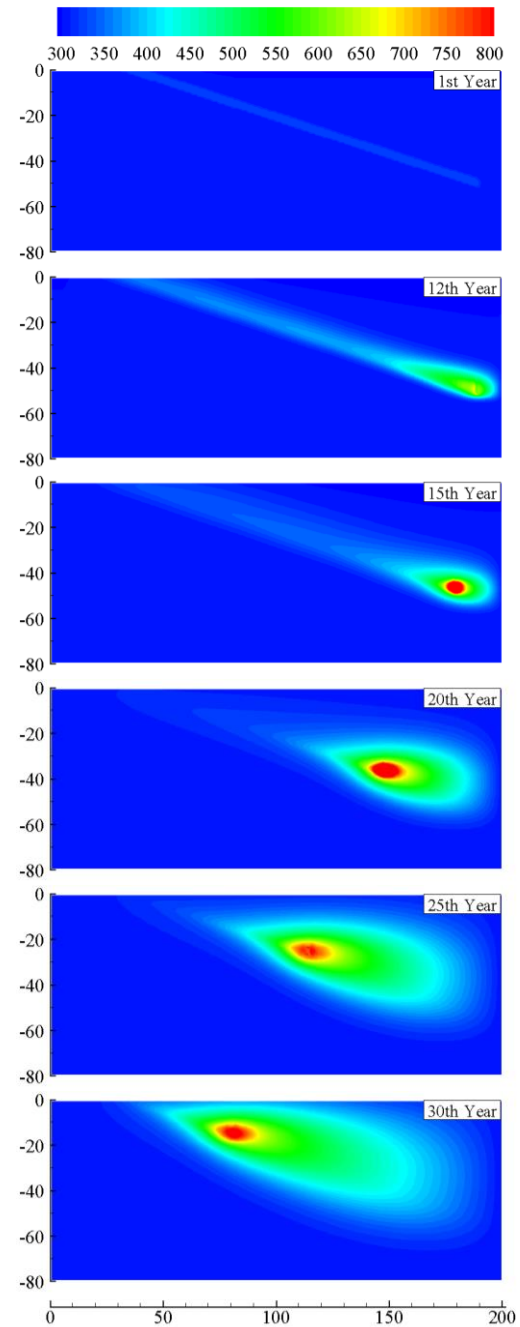


FIG. 3. Time-depended slices of simulated temperature profile in coal fire history.

### Oxygen and fuel consumption

In order to comprehensively reveal the self-ignition and fire propagation in the coal seam, especially the relativity between the combustion, oxygen and coal consumption processes, the coal fire development is divided into two periods including early ignition and stable combustion.

For the first period, the temperature, oxygen content and local coal consumption distributions from the first to eleventh

year after coal opening up are plotted in Figs. 4, 5 and 6, respectively.

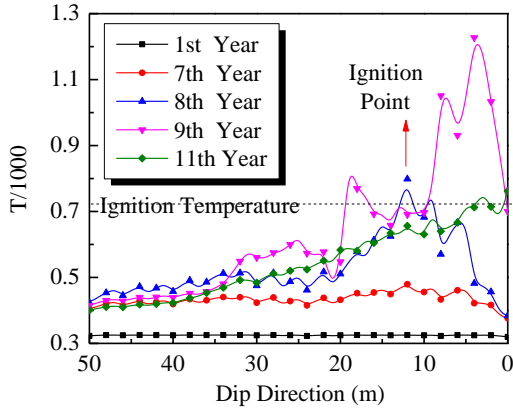


FIG. 4. Temperature distributions during the early oxidation stage in the coal seam.

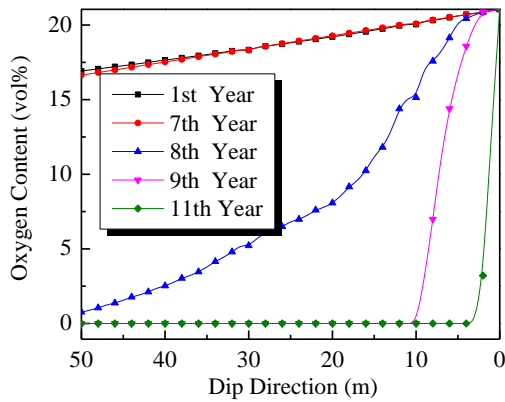


FIG. 5. Oxygen consumption characteristics by chemisorption along the dip direction.

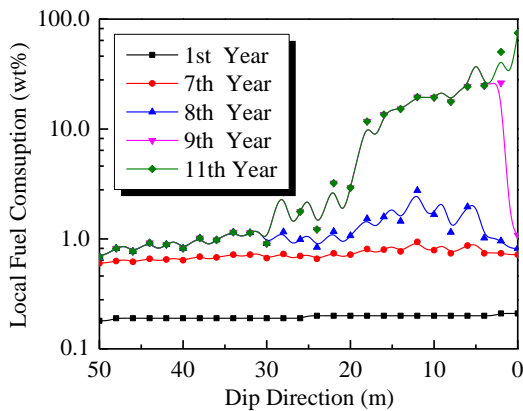


FIG. 6. Fuel consuming variations after different oxidizing period.

In Fig. 4, it is seen that since coal opened up, the seam temperature gradually and slowly rises with the coal oxidation process, the increasing temperature at the interface between goaf and seam is lower than that in the inner area nearby due to the

convection heat transfer to the downstream caused by leakage air until 8<sup>th</sup> year. After that, the temperature at about 12 m in the dip direction goes beyond the critical temperature and combustion starts. Noticing the same position and time in Fig. 5, it can be seen that the initial ignition is under the lack oxygen condition (about 15 vol%). However, the original combustion could not keep at certain position but move to up- and downstream in the next year. Even two years later, the coal temperatures along the whole seam drop to under the ignition critical value except the area near the goaf.

The oxygen and coal consumption characteristics during early oxidation period illustrated in Figs. 5 and 6 could explain this strange and non-monotonic variation. Before the eighth year, oxygen supplement with the leakage air could match the oxygen requirement of coal reaction at low temperature that leads the oxygen content is linear decreasing in the dip direction with synchronous oxidizing through the coal seam (cf. Fig. 5). At the same time, there exists a slight and nearly same fuel consumption along the whole seam by coal chemisorption with enough oxygen (cf. Fig. 6). It indicates that, during this stage, the thermodynamic process of spontaneous combustion is mainly dominated by reaction rate and heat release of coal oxidation.

When the temperatures around 12 m in the dip direction exceed the ignition temperature at the end of eighth year, local oxygen consumptions sharply enhance with the occurrence of severe reactions of fuel combustion near there. And then, this dramatically change causes a rapid drop in local oxygen concentrations and the lean oxygen environment occurs after original ignition. Without oxygen supplement, the remained coals stop reaction around the ignition point after the ninth year except the coals near the interface between the seam and the goaf with continuous combustion under enough oxygen supply from the fractures.

When the bottom coals burnout after the eleventh year, the oxygen starts to seep into deep seam and re-ignitions occur in the original combustion zone, so that the combustion state changes from the early oxidation to stable movement or development. Figs. 7-9 plot the temperature, oxygen content and local coal consumption distributions in the dip direction at 15<sup>th</sup>, 20<sup>th</sup>, 25<sup>th</sup> and 30<sup>th</sup> year, respectively. It is seen in Fig. 7 that the maximum temperatures at different times are ranging from about 950 K to 1100 K while all the intervals between the peaks stay at a relatively fixed value. The combustion zone moves towards the outcrop with a stable rate of fire propagation.

Moreover, comparing the oxygen contents and local fuel consumption (cf. Figs. 8-9), a step variation along the seam dip is recorded at any time for the both values. In detail, the position of entire loss falls a little bit behind the position of oxygen concentration decreasing. This synchronous changing means that the oxygen is the dominated factor for the fire propagation in this stage of stable combustion. Due to very fast reaction kinetics at high temperatures, immediate consumption of all the oxygen takes place within the combustion center. Combustion will only proceed when transport processes provide further oxygen.

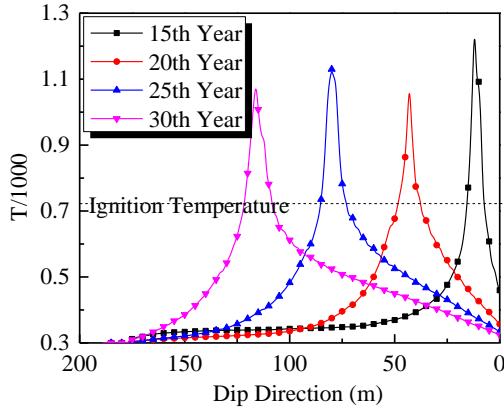


FIG. 7. Temperature distributions after ignition in the coal seam.

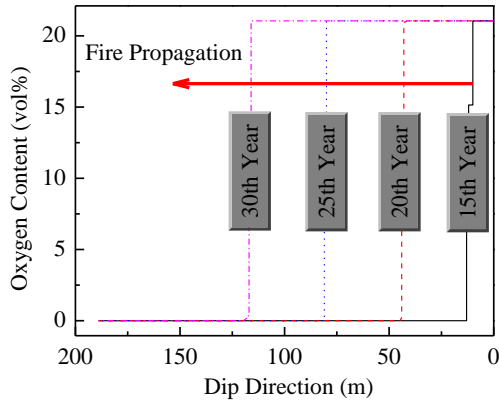


FIG. 8. Oxygen contents in the dip direction after different combustion period.

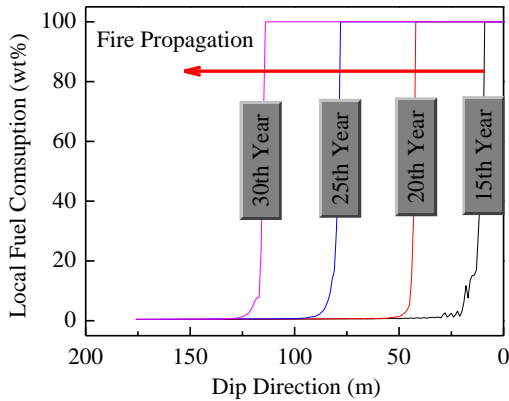


FIG. 9. Local fuel consuming variations along the coal seam until 30<sup>th</sup> year.

### Analysis of influencing factors

As mentioned above, chemical and physical parameters involved in the simulation have significant influences on the fire development. Here, three kinds of geophysical factors including

inclined angle of dip, fracture width of leakage channel and porosity in the coal seam are taken into consideration.

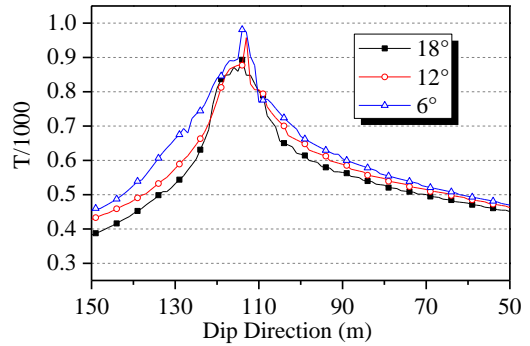


FIG. 10. Simulated temperature distributions with variation of dip angle.

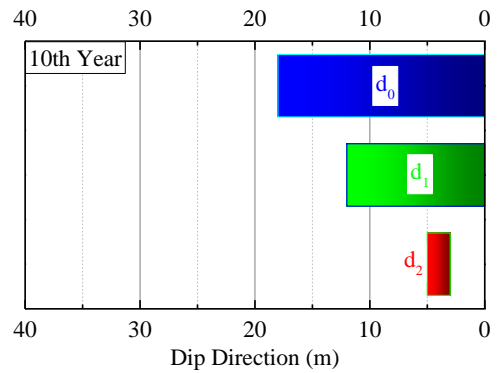


Figure 11.

FIG. 11. Combustion zones with different simulated fracture widths after 10<sup>th</sup> year (Width  $d_0$ :10cm,  $d_1$ :5cm and  $d_2$ :1cm).

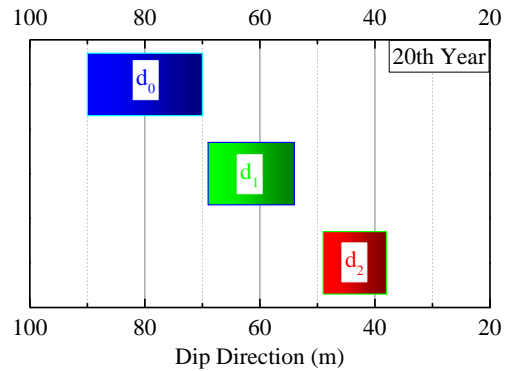


FIG. 12. Combustion zones with different simulated fracture widths after 20<sup>th</sup> year (Width  $d_0$ :10cm,  $d_1$ :5cm and  $d_2$ :1cm).

Fig. 10 plots the simulated temperature distributions along the seam dip with different inclined angle after 30<sup>th</sup> year since coal opened up. It is seen that with inclined angle of 6°, the combustion peak is slightly in front of the other two peaks towards the outcrop and the hotspots zone is also larger than the others. It indicate that when the inclined angle decreases from 18° to 6°, the fire propagation rate becomes a little bit fast. This

phenomenon shall be due to the enlarged contact area between the coal and oxygen at the same horizontal level with lower inclined angle, then more heat of coal reaction releases at early oxidizing stage.

Considering the effects of fracture width of leakage channel that could represent the leakage intensity, the simulations are repeatedly operated with 10 cm, 5 cm and 1 cm in width, respectively. As shown in Figs. 11 and 12, the simulated combustion zone with fracture width of 10 cm performs in a significant larger area than that with the other two widths. Especially, the last result with widths of 1 cm proves that the seam is experiencing the initial ignition process in early oxidation stage, which means the fire development in this circumstance is pretty slow. After ten years, the differences between the combustion zones are much more obvious, in which the positions of fire center with fracture width of 10 cm, 5 cm, and 1 cm are observed at about 80 m, 62 m and 43 m in the dip direction, respectively. In addition, the length of combustion zone with larger fracture width is larger. It illustrates that with decreasing of fracture width, the leakage air seeping into the seam changes smaller within the same interval time, and then the lower leakage intensity significantly influences the propagation rate of coal fire towards to the outcrop.

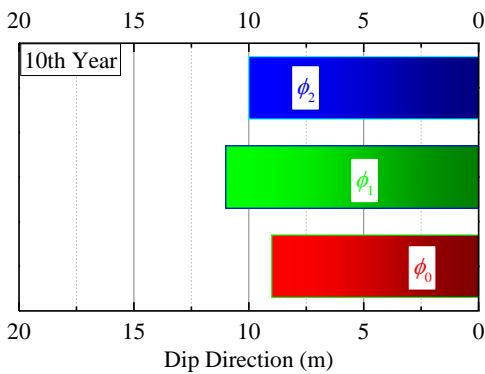


FIG. 13. Effects of porosity on combustion zones with variation of porosity in 10<sup>th</sup> year.

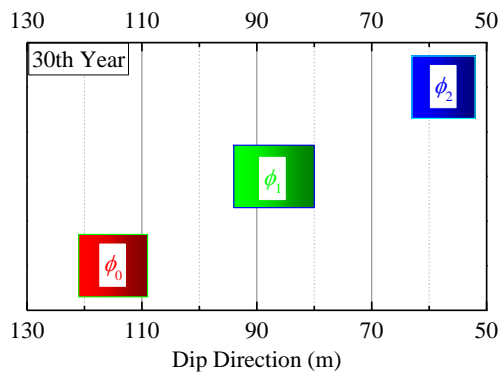


FIG. 14. Effects of porosity on combustion zones with variation of porosity in 30<sup>th</sup> year).

Furthermore, as an important geological factor, the porosity in the stratum is also taken into consideration in this section. Here, three porosities  $\phi_0$ ,  $\phi_1$  and  $\phi_2$  of 0.2, 0.15 and 0.1 in the seam are assumed and implemented in the simulation,

respectively, and the other strata keep their porosities invariably. Comparative results find an almost constant combustion zone of about 10 m in length at the seam bottom in the 10<sup>th</sup> year with different porosities. It means at the early oxidizing stage, enough oxygen supplement lead the processes of coal oxidation and heat release are independent of coal porosity. But when it changes to the stable state of fire movement in 30<sup>th</sup> year, the reactions are entirely controlled by the oxygen supply which determined by the leakage flow, so the higher porosity with higher seepage velocity in the porous medium results in more oxygen transfer and a faster rate of fire propagation.

## FIELD APPLICATION

### Brief of coal fire history

Heshituoluogai coal fire is located in the Hoboksar Mongol Autonomous County, northwest of the Junggar Basin. There are 12 sub-fire areas caused by improper mined post-processing, distributed in a range of 57 km<sup>2</sup> as drawn in Fig. 15. The earliest coal fires occurred in the 1<sup>#</sup>, 2<sup>#</sup> and 3<sup>#</sup> fire areas in 1968, and then during the period from 1968 to 1990, other six areas observed the spontaneous combustion. The 8<sup>#</sup> area, igniting in September 2008, is the latest coal fire. Since 2000, the county government has repeatedly and costly operated fire extinguishing many times, but the fires have not been controlled with lack of water near the fire areas as well as the effective extinguishing methods. Instead, the advance rate of fire front greatly accelerates with the expansion of leakage channel in underground burning body.

Among these 12 sub-fire areas, the fifth fire area has the greatest impact on coalmine safety production. It is about 130 m apart from No.9 well belonging to Xuzhou mining group co., LTD in southeast. Since the mining level of the well is a few meters higher than the burning bottom of fire area, so that it has been seriously threatened by the rapid movement of self-combustion along the seam. To this end, the in-situ study presented here was conducted in the fifth fire area. This fire area started burning in 1986, due to the spontaneous combustion of coal in abandoned mine goafs after the old mine shutdown which was built in 1965 with 7 wells. The underground goafs of wells No.3 to 6 were fully connected and the spontaneous combustion was firstly observed in well No.5 where the gas temperature passed 38°C and carbon monoxide was found in the roadway. All the wells closed in 1986 and fire features at surface upper the No.4 and 6 wells were identified in the following years.

The fifth fire area is located at about 7 km southwest of the town of Heshituoluogai, next to the G217 National Road (cf. Fig. 15). The center point coordinates of the fire area are located at 85°, 58 min east longitude and 46°, 27 min north latitude. For field survey in 2011 year, control survey of fire area is based on the national four degree points WQN, 125, 128 and 83409, control network is set by using GPS static mode with the fitting elevation. According to a surface temperature survey, the northern area has a higher surface temperature, and the highest temperature measured on the surface is 674°C (cf. Fig. 15). In addition, through the temperature reduction, the

temperature range of fire area by infrared measurement is 23°C to 160°C with a zonal distribution of high temperatures.

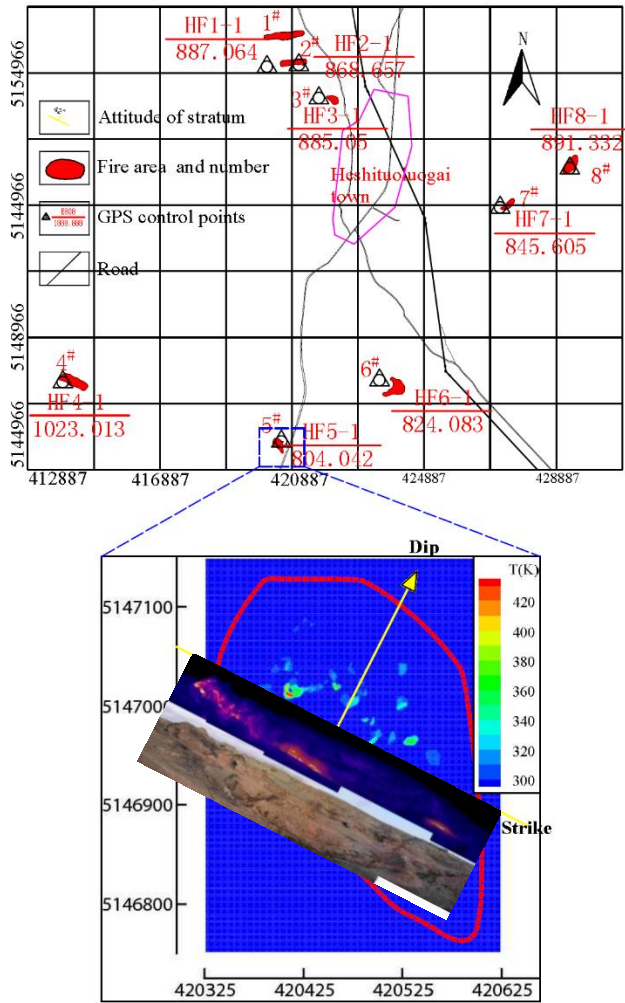


FIG. 15. Area chart of Heshituoluogai coal fires, surface temperature map and infrared photo for the fifth fire area.

### Coal loss estimation

The geologic units covering of the fifth fire area consist of Devonian, Carboniferous, Jurassic, Tertiary and Quaternary. The coal-bearing stratum is the upper Badaowan Formation of the Lower Jurassic ( $J_1B^2$ ), the thickness of stratum varies from 109.61 to 221.54m with an average value of 161.22 m. There are 8-12 coal seams contained in the Badaowan Formation, numbered from the bottom  $A_1$  to  $A_{12}$ . All of the 12 coal seams are long-flame or jet coal (brand CY41) with weak caking index. The main recoverable and combustion coal seams are  $A_2$ ,  $A_3$  and  $A_4$  with stable development district and the rest seams are unrecoverable or local minable. Average thickness of all the coal seams is 12.12 m with coal-bearing coefficient of 8.20%. Some portions of the seam  $A_2$  and  $A_3$  merge into one layer and  $A_4$  is very close to the other two seams, therefore these three seams are regarded as one layer in the simulation with an average total

thickness of 7.99 m, strike direction of 27° and dip angle of 18° (cf. Fig. 15). The relative density of coals sampling from  $A_2$ ,  $A_3$  and  $A_4$  are 1410, 1320 and 1300  $kgm^{-3}$ , respectively; thus, an averaged value of 1340  $kgm^{-3}$  is employed in the simulation. Then, the fire bottom or worked-out floor is 738 m from the seal level and the surface elevations vary from 798 m to 808 m, therefore, the buried depth of seam bottom is about 60 m. Other thermal, chemical and physical parameters employed in the evaluation follow the settings in Section 2.3, and simulation results are drawn in Figs. 16 and 17.

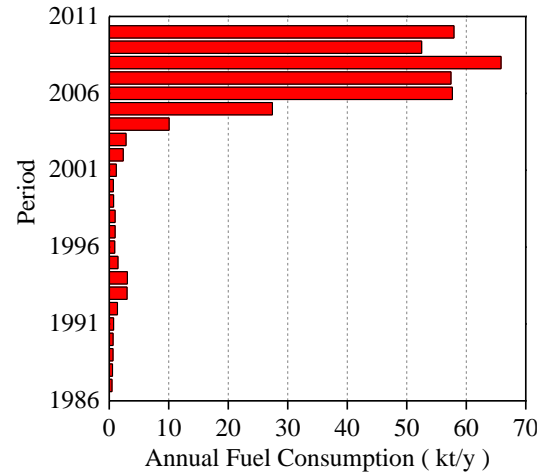


FIG. 16. Annual consumption of coal reserves during the period from 1987 to 2010.

Figure 16. Annual consumption of coal reserves during the period from 1987 to 2010.

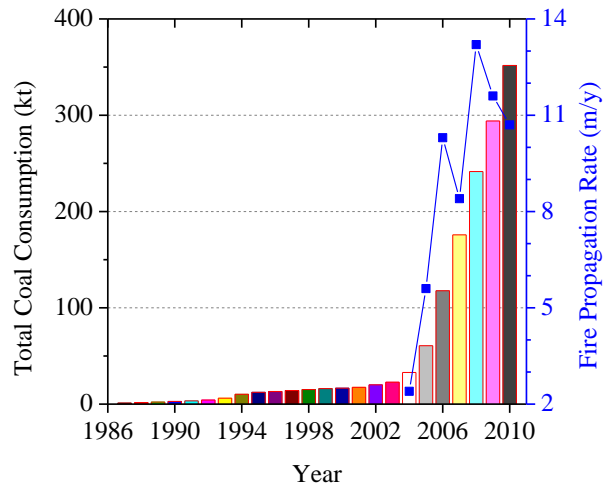


FIG. 17. Accumulated coal loss and fire propagation rate during the period from 1987 to 2010.

Fig. 16 plots the annual coal consumptions from 1987 after the old mine shutdown in the year 1986 until 2010. The original reserves loss by self-combustion reads 460 tons in 1987 and then it increases to about 3 kilo tons around the year 1994 due to the original oxidation and ignition at early oxidizing stage. After that time, the combustion is restrained under lean oxygen supply for

a long time so that the annual fuel consumption stays a lower level in the following several years until 2003. In the next year, the coal loss dramatically enlarge to about 10 kilo tons and continuously increase to around 60 kilo tons in 2006 and keep a high level as so far.

Moreover, the accumulated reserves loss from the seam opened up is recorded simultaneously as shown in Fig. 16. It indicates that the total coal loss till 2010 achieves more than 350 kilo tons. Meanwhile, the simulated propagation rate of coal fire varies from 8 m to 13 m per year in the latest five years with average rate of 10.8 m per year. Considering the rest coals in the outcrop seam and the movement of combustion front, the occurrence reserves in the whole outcrop will be entire consumed by the end of year 2022 or 2023

In practice, there are two indirect methods which could rough estimate the loss reserves except simulation, one is gas production tracing [25] and the other is surface heat evaluation [26].

For the first method, the tests of gas sampling and point positioning are operated in field synchronously. NOVAH8 gas monitor was employed in the measurement, and the precisions of gas concentration and velocity are 0.1 PPM and 0.1 m/s. After observing all the gas exhaust vents at surface of fire area, gas emissions could be determined by multiplying the gas concentration, flow velocity and crack area. According to the greenhouse gas emissions, the oxygen consumption could be revised and the fuel loss is calculated by theoretical oxygen requirement mentioned in section 2.1. Based on the field data in 2010, the carbon dioxide emission each year from the Hestuluogai fire area approximates 2.2 million tons and it reads about 128.3 kilo tons from the fifth fire area. In this way, the speculative annual loss of coal reserves in 2010 is 46.8 kilo tons.

On the other hand, based on thermal equilibrium theory, the evaluation process for combustion loss of coal reserves in fire area describes as follows. The hot points at surface are identified firstly by using surface temperature measurement and the contours of temperature distribution are delineated by Surfer software. And then, the areas of different temperature ranges are counted and the heat release into the atmosphere every year for each temperature level is determined according to the coefficient of heat transfer depending the difference between surface temperature and the annual averaged air temperature of the fire area region. Summing these values up, the total heat release could be obtained and divide it by net calorific value of coal, the annual loss of coal reserves is finally determined. In this way, according to the detailed prospecting data reported by Xinjiang Coal Fire Fighting Bureau [10], the total area of fire delineation approximates 84,013m<sup>2</sup> with annual combustion loss of 95.5 kilo tons, burnout coal achieves 1.061 million tons till the end of year 2010 and the threatening reserves beyond 3.6 million tons.

Back to the simulation results, it is read in Fig. 16 that the simulated annual coal loss in 2010 is 57.9 kilo tons and the averaged value from 2006 to 2010 is 58.3 kilo tons. This loss reserves is less than the value evaluated by the heat release but higher than that revised from gas emission. In fact, the estimation method with heat release often exaggerates the temperature

ranges especially the hotspots leading to a bigger result. On the contrary, the prediction by gas emissions misses the residual carbon left in the seam and a small amount of gases exhausting from the soils, so that it may present a smaller result. Comparing the simulation with these two indirect observations, it can concluded that simulated results is closer to the true value and it is an effective method for the loss estimation in coal fire development.

## CONCLUSIONS

This work focuses on the loss estimation of coal reserves caused by spontaneous combustion in coalfield fire areas. Combined with quantitative modelling for the correlations between coal/oxygen consumption and reaction heat release, a coupled heat and mass transfer model for inclined outcrop seam in porous coal-bearing strata with transient exothermic source term is established. The main conclusions are drafted as follows.

By tracing the variations of temperature, oxygen concentration and local fuel consumption along the long-term history of coal fire, simulated data indicate that the combustion or heat release rate is therefore controlled by reaction kinetics at low temperatures due to the slower oxygen consumption, but reaction kinetics become very fast at high temperatures and oxygen transport controls the overall combustion rate. Considering the variation of influence factors, comparative analyses illustrate that fire movement changes slightly faster with lower inclined angle, then the propagation rate and fuel loss are significantly and positively related to the fracture width or leakage intensity while reduced when the stratum porosity decreases. For the field application, the estimation results show that the annual reserves loss by self-combustion is around 60 kilo tons with an averaged propagation rate of 10.8 m per year for the fifth fire area of Heshituoluogai coal fires. And in this way, the whole outcrop seam would be totally lost till 2022 or 2023. Comparing the simulated results with the other two indirect methods, it illustrates that the simulation model could predict better coal loss.

## ACKNOWLEDGMENTS

This research was supported by the Outstanding Youth Science Foundation of NSFC (No. 51522601) and Program for New Century Excellent Talents in University (NCET-13-0173). Y.M. Wang appreciates the Scholarship provided by the Chinese Scholarship Council to study at Rutgers University.

## REFERENCES

- [1] Kuenzer, C., Zhang, J., Tetzlaff, A., 2007, Uncontrolled coal fires and their environmental impacts: Investigating two arid mining regions in north-central China, *Applied Geography*, **27**(1), pp. 42–62.
- [2] Chatterjee, R.S., 2006, Coal fire mapping from satellite thermal IR data—a case example in Jharia Coalfield, Jharkhand. *ISPRS Journal of Photogrammetry and Remote Sensing*, **60**(2), pp. 113–128.

- [3] Whitehouse, A.E., Mulyana, A.A.S., 2004, Coal Fires in Indonesia, *International Journal of Coal Geology*, **59**, pp. 91–97.
- [4] Heffern, E.L., Coates, D.A., 2004, Geologic history of natural coal-bed fires, Powder River basin, USA, *International Journal of Coal Geology*, **59**, pp. 25–47.
- [5] Nolter, M.A., Vice, D.H., 2004, Looking back at the Centralia coal fire—a synopsis of its present status. *International Journal of Coal Geology*, **59**, 99–106.
- [6] Pone, J.D.N., Hein, K.A.A., Stracher, G.B., Annegarn, H.J., Finkelman, R.B., Blake, D.R., 2007, The Spontaneous Combustion of Coal and Its By-products in the Witbank and Sasolburg Coalfields of South Africa, *International Journal of Coal Geology*, **72**, pp. 124–140.
- [7] Song, Z., Kuenzer, C., 2014, Coal fires in China over the last decade: a comprehensive review. *International Journal of Coal Geology*, **133**, pp. 72–99.
- [8] Xinjiang Coal Field Fire-Fighting Engineering Bureau, 2009, *The Third Survey Report on the Coal Fires in Xinjiang Uygur Autonomous Region*. (In Chinese)
- [9] Stracher, G.B., Taylor, T.P., 2004, Coal Fires Burning Out of Control Around the World: Thermodynamic Recipe for Environmental Catastrophe, *International Journal of Coal Geology*, **59**, pp. 7–17.
- [10] Xinjiang Coal Field Fire-Fighting Engineering Bureau, 2010, *Detailed prospecting report on the coal fire areas in Heshituoluogai*. (In Chinese)
- [11] Rosema, A., Guan, H.Y., Veld, H., 2001, Simulation of Spontaneous Combustion to Study the Causes of Coal Fires in the Rujigou Basin, *Fuel*, **80**, pp. 7–16.
- [12] Wessling, S., Kuenzer, C., Kessels, W., Wuttke, M.W., 2008, Numerical Modeling for Analyzing Thermal Surface Anomalies Induced by Underground Coal Fires, *International Journal of Coal Geology*, **73**, pp. 175–184.
- [13] Yip, K., Ng, E., Li, C.Z., Hayashi, J.I., Wu, H.W., 2011, A Mechanistic Study on Kinetic Compensation Effect During Low-Temperature Oxidation of Coal Chars, *P. Combust. Inst.*, **33**, pp. 1755–1762.
- [14] Zarrouk, S.J., O'Sullivan, M.J., 2006, Self-heating of Coal: the Diminishing Reaction Rate, *Chem. Eng. J.*, **119**, pp. 83–92.
- [15] Mazumdar, B.K., 2000, Thermochemical history in the genetic path of coal: derivation of a novel correlation for the heat of combustion, *Fuel*, **79**, pp. 1267–1276.
- [16] Jones, J.C., Henderson, K.P., Littlefair, J., Rennie, S., 1998, Kinetic Parameters of Oxidation of Coals by Heat-release Measurement and their Relevance to Self-heating Tests, *Fuel*, **77**, pp. 19–22.
- [17] Ozbas, K.E., Kök, M.V., Hicyilmaz, C., 2003, DSC Study of the Combustion Properties of Turkish Coals, *J. Therm. Anal. Calorim.*, **71**, pp. 849–856.
- [18] Mazumdar, B.K., 2000, Theoretical Oxygen Requirement for Coal Combustion: Relationship with Its Calorific Value, *Fuel*, **79**, pp. 1413–1419.
- [19] Liu, M.X., Shi, G.Q., Guo, Z.X., Wang, Y.M., Ma, L.Y., 2016, 3-D Simulation of Gases Transport under Condition of Inert Gas Injection into Goaf, Heat Mass Transfer. <http://dx.doi.org/10.1007/s00231-016-1775-8>.
- [20] Wang, Y.M., Shi, G.Q., Wang, G.Q., 2013, Numerical Study on Thermal Environment in Mine Gob under Coal Oxidation Condition, *Ecol. Chem. Eng. S*, **20**, pp. 567–578.
- [21] Shi, G.Q., Liu, M.X., Wang, Y.M., Wang, W.Z., Wang, D.M., 2015, Computational Fluid Dynamics Simulation of Oxygen Seepage in Coal Mine Goaf with Gas Drainage, *Math. Probl. Eng.*, Article ID 723764, 9 pages. <http://dx.doi.org/10.1155/2015/723764>.
- [22] Zeng, Q., Tiyyip, T., Wuttke, M.W., Guan, W.M., 2015, Modeling of the Equivalent Permeability for an Underground Coal Fire Zone, Xinjiang Region, China, *Nat. Hazards*, **78**, pp. 957–971.
- [23] Shao, Z.L., Wang, D.M., Wang, Y.M., Zhong, X.X., 2014, Theory and application of magnetic and self-potential methods in the detection of the Heshituoluogai coal fire, China. *Journal of Applied Geophysics*, **104**, pp. 64–74.
- [24] Li, B., Chen, G., Zhang, H., Sheng, C., 2014, Development of Non-isothermal TGA-DSC for Kinetics Analysis of Low Temperature Coal Oxidation Prior to Ignition, *Fuel*, **118**, pp. 385–391.
- [25] Fierro, V., Miranda, J.L., Romero, C., Andrés, J.M., Pierrot, A., Gómez-Landesa, E., Arriaga, A., Schmal, D., 1999, Use of infrared thermography for the evaluation of heat losses during coal storage, *Fuel Processing Technology*, **60**(3), pp. 213–229.
- [26] O'Keefe, J.M.K., Neace, E.R., Lemley, E.W., 2011, Old Smokey coal fire, Floyd County, Kentucky: Estimates of gaseous emission rates. *International Journal of Coal Geology*, **87**, pp. 150–156.